

# Avalanche Photodiodes Performance Parameters Estimation under Thermal Irradiation Fields

Ahmed Nabih Zaki Rashed<sup>1</sup>, Abd El-Naser A. Mohamed<sup>1</sup>, Imbaby I. Mahmoud<sup>2</sup>,  
Mohamed S. El\_Tokhy<sup>2</sup>, and Osama H. Elgzar<sup>2</sup>

<sup>1</sup>Electronics and Electrical Communication Engineering Department,  
Faculty of Electronic Engineering, Menouf 32951, Menoufia University, EGYPT

<sup>2</sup>Engineering Department, Nuclear Research Center, Atomic Energy Authority, P.O. 13759, Inshas, EGYPT

**Abstract—** Radiation-induced damage in Avalanche Photodiode (APD) was shown to result from the dark current and a change of the effective doping concentration occurring within the photodiodes. In this paper a model to reveals the effect of ionizing radiation and temperature on the performance of APDs is built by using Vissim environment. This proposed model provides a mean to control the properties of APD when they are selected to operate in thermal radiation environments. Efficiency, sensitivity, responsivity, detectivity, noise equivalent power, excess noise factor, normalized detectivity, and signal to noise ratio are modeled. The temperature effects are combined with radiation effects to formulate a rigorous treatment for the APD behavior. The results are validated against published experimental work in temperature case and show good agreement.

**Index Terms—** APD, Radiation effects, Excess noise factor, Noise equivalent power, Responsivity, and Detectivity .

## I. INTRODUCTION

Optoelectronic components have become important elements in modern electronic systems due to the many intrinsic advantages of optical signal transfer, especially the large available bandwidths, high immunity to electromagnetic interference, and light weight [1]-[6]. Among of these components is the photodiode which when is exposed to the effects of light, then the photon energy is used to break the covalent bond releasing electrons and creating a hole in the process. If the generation of electrons and holes occurred in the depletion area, then the existing electric field removes them from that area before they get a chance to recombine. As a result, the reverse current (photocurrent) occurs. Photocurrent grows in proportion to the intensity of light. For larger values of reverse bias voltage photocurrent does not depend on the applied voltage but is practically constant. The number of generated electron-hole pairs increases only with the increasing of the light intensity [7]. Moreover the designer has three basic detector choices - the silicon PIN detector, the silicon avalanche photodiode (APD) and the photomultiplier tube (PMT) [8]. However at best, a pin diode can generate only one electron-hole pair per incident photon and therefore a pre-amplifier is needed for low light level detection. This limitation can be overcome by using (APDs) [2]. They operate by converting clusters of detected photons, associated with information-carrying pulses of light in a digital communication system, into cascades of electrons. These cascades have sufficiently high charge to be readily detected by the electronics following the APD [9]. Furthermore their high sensitivities have recently led them to be widely used in high-radiation environments [9]-[12], which include reactors and the space environments. Therefore the radiation sources influence the APD properties can be neutrons, gamma [13]. However the main problem is caused by the neutron radiation when the new photodetector prototypes have been used [14]. Since neutron irradiation is believed to cause large clusters of

disorder (defects) in the crystal lattice which leads to increase dark current as well as noise and thus raise the minimum detectable light power [15]-[18]. The other important permanent damage effect is a change of the effective doping concentration (Neff) that will modify the avalanche gain behavior of the APD. Such defects could also act as trapping centers and cause a change of APD parameters such as the change collection efficiency and quantum efficiency and a reduction in optical sensitivity [5], [15],[19]-[21].

Thus, it is important to know the properties of the APDs in the irradiation environment, and how we can optimize these properties in order to improve APDs characteristics. Consequently, we are concerned with radiation effects on device efficiency, responsivity, sensitivity, dark current and excess noise factor which enables us to calculate the humilitation that occurs in APDs performance under irradiation environment. In addition, this allows improving the detectivity, noise equivalent power, and signal to noise ratio which contributes in achieving maximum usage of the communication system bandwidth and to control APDs properties in radiation environments. The arising effects of radiation induced damage are decisive in designing high-bit-rate optical communication systems. This work is done by using VisSim environment. VisSim is a visual block diagram language for simulation of dynamical systems and model based design of embedded systems. It uses a graphical data flow paradigm to implement dynamic systems based on differential equation. This paper is organized as follows: Section II presents the basic assumptions and modeling of radiation induced damage, section III describes the model results. However section IV is devoted to conclusion.

## II. BASIC ASSUMPTIONS AND MODELING OF RADIATION INDUCED DAMAGE

In this model two Avalanche photodiodes were used, one of effective thickness =140  $\mu\text{m}$  and the other is equal to 120 $\mu\text{m}$  and the photodiodes are assumed to overfill the fiber so that all mode groups are received. The cross sectional areas diameters of the two devices are 0.8 and 0.5 mm. Operating wavelength of the optical sources used for transmitting data is 850 nm. To illustrate the optical responses of avalanche photodiode in radiation environment, the effect of the neutron radiation on the properties of avalanche photodiodes such as Detectivity and Noise Equivalent Power has been studied under different thermal condition. Consequently we should reveal the harmful neutron radiation effect that has two main contributions to the dark current of an APD. The first of these is the surface dark current, generated at or near of the perimeter of the junction. This current occurs outside the multiplying region, and is therefore not multiplied. The second contribution to the dark current is bulk current, generated within the

junction region, and in an APD this current component undergoes multiplication. Thus we have [8].

$$I_D = I_{DS} + MI_{DB} \quad (1)$$

Where  $I_D$ ,  $I_{DS}$ ,  $I_{DB}$ , and  $M$  are a the total dark current, the unmultiplied surface component of the dark current, the multiplied component of the dark current, and multiplication factor (gain) respectively. Moreover the dark current resulted from neutron effect can be also obtained as [22].

$$I_{Dark\ neutron} \cong I_{Dark\ gamma} - I_{Dark\ proton} = MI_{DB} \quad (2)$$

Therefore equation (1) can be simplified as follows:

$$I_D = I_{DS} + I_{Dark\ neutron} \quad (3)$$

However, under neutron fluence  $\Phi$  the dark current is a volume effect, so usually the increase in the dark current  $I_{Dark\ neutron}$  is written as follows [14].

$$I_{Dark\ neutron} = \alpha v \Phi \quad (4)$$

where  $v$ ,  $\alpha$  are the volume of the detector, and a parameter which has been measured by different groups, and its value is ranging between  $\alpha = (10-13)10^{-17} \text{A/cm}$ . In the case of Avalanche Photodiodes, the volume which is relevant for the generation of the bulk current is the area times the effective thickness of the detector [14].

$$v = A_d \times T_E \quad (5)$$

Therefore equation (3) can be rewritten as follows:

$$I_D = I_{DS} + \alpha v \Phi \quad (6)$$

Moreover one of important characteristics that are commonly used to describe photodetector performance is the quantum efficiency ( $\eta$ ) that can be defined as the ratio of number of incident photon to the face of photodiode in unit time and is denoted as ( $N_p$ ) to the number of photoexcitation photoelectron ( $N_e$ ). Then the quantum efficiency  $\eta$  is defined as [23]:

$$\eta = \frac{N_e}{N_p} \times 100\% \quad (7)$$

Where

$$N_e = \frac{I_{ph}}{q}, \quad N_p = \frac{P\lambda}{hc} \quad (8)$$

where  $P$  is physical radiated power of the incident light,  $I_{ph}$  is the photo-current which produced in photodiode when the radiated power is  $P$ . Thus, Substitute (8) into (7), we have [23].

$$\eta = \frac{I_{ph}hc}{q\lambda P} \times 100\% \quad (9)$$

Where  $\lambda$ ,  $h$ ,  $q$ , and  $c$  is incidence light wavelength, Planck constant ( $6.626 \times 10^{-34} \text{J}\cdot\text{S}$ ), electric charge, and light velocity respectively. Furthermore from equation (9) we obtain the relationship between photogenerated current  $I_{ph}$  and optical power  $P$  in photodiode [23]

$$I_{ph} = \frac{\eta q \lambda}{hc} P \quad (10)$$

In addition when the wavelength of incident light (light source) and photosensitive device (material) are fixed the value of  $(\eta q \lambda / hc)$  is constant. Consequently we can write the photodiode sensor's responsivity  $S_R$  as in the following equation [23]

$$\frac{I_{ph}}{P} = \frac{\eta q \lambda}{hc} \quad (11)$$

So we can suppose that [23]

$$S_R = \frac{\eta q \lambda}{hc} \quad (12)$$

Substitute  $S_R$  into (10), then we obtain [23]

$$I_{ph} = S_R P \quad (13)$$

Thus, the responsivity is essentially a measure of the effectiveness of the detector for converting electromagnetic radiation to electrical current or voltage. Furthermore equation (9) can be written as the following [23]

$$\eta = S_R \frac{hc}{q\lambda} \quad (14)$$

Moreover, the quantum efficiency  $\eta$ , can be also calculated from the formula [11]

$$\eta = S_I \frac{hc}{q\lambda} \quad (15)$$

Where  $S_I$  is the primary photoelectric sensitivity of avalanche photodiodes which can be calculated from the equation [11]

$$S_I = \frac{I_{ph}}{P} = \frac{\eta q \lambda}{hc} \quad (16)$$

Consequently, from eqs. (12), (16) we can conclude that:

$$S_I = S_R \quad (17)$$

However, the total sensitivity is related to the primary sensitivity by the following equation [11]

$$S_T = M S_I \quad (18)$$

Furthermore, from equation (17) the total sensitivity is related to the responsivity by the following equation

$$S_T = M S_R \quad (19)$$

So that responsivity gives a measure of the detector's sensitivity to radiant energy. Moreover another important characteristic used to describe photodetector performance is the signal to noise ratio (S/N ratio) that can be determined for APDs by the equation [24]:

$$\frac{S}{N}(M) = \frac{M^2 I_{ph}^2}{2qB \left[ I_{ph} M^2 F(M) + \left( I_{DS} + I_{DB} M^2 F(M) \right)^2 \frac{(T-300)/10}{10} \right] + \frac{4kTB}{R_L}} \quad (20)$$

Where  $k$ ,  $T$ ,  $B$ ,  $R_L$ , and  $F(M)$  are the Boltzman's constant, temperature, load resistance, and excess noise factor respectively. However the excess noise factor may be calculated using the model developed by McIntyre which considers the statistical nature of avalanche multiplication. Thus the excess noise factor is given by [8]

$$F(M) = K_{EFF} M + \left[ 1 - K_{EFF} \left( 2 - \frac{1}{M} \right) \right] \quad (21)$$

Where  $K_{EFF}$  is the effective k-factor for an APD, whereas k-factor is the carrier ionization ratio. Furthermore in equation (20) the first component in the denominator describes the shot noise ( $N_{sh}$ ) but the second one the thermal noise ( $N_{th}$ ) of the load resistance. So that from equation (20) the shot noise can be calculated from the equation [24]

$$N_{sh} = 2qB \left( I_{ph} M^2 F(M) + I_{DB} M^2 F(M) \right) \quad (22)$$

Moreover shot noise is present in all photon detectors due to the random arrival rate of photons from the source of radiant energy under measurement and background radiation. This shot noise is the true ultimate limitation to detector performance. However, the thermal noise can be calculated from the equation [24]

$$N_{th} = \frac{4kTB}{R_L} \quad (23)$$

It occurs in all conducting materials. It's a consequence of the random motion of electrons through a conductor. The electrons are in constant motion, but they collide frequently with the atoms or molecules of the substance. Each free flight of an electron constitutes a minute current. The sum of all these currents taken over a long period of time must, of course, be equal to zero. But their ac component is thermal noise. Therefore the total noise ( $N_T$ ) can be calculated from the following equation [24]

$$N_T = N_{sh} + N_{th} \quad (24)$$

Moreover a substantial characteristic for an avalanche photodiode is dependence of a multiplication factor ( $M$ ) on its reverse bias voltage. Therefore an empirical relationship describes this characteristic for parametrically variable temperature is given by [24].

$$M(V, \Phi, T) = \frac{H}{V_b + [0.18(300 - T)] - V_R} \quad (25)$$

Where  $V_b$ ,  $V_R$ ,  $T$  are the breakdown voltage, and the reverse bias voltage, and ambient temperature respectively. In addition an approximate universal expression of the breakdown voltage for all semiconductors studied can be given as follows [25].

$$V_b = a \left[ \frac{E_g}{1.1eV} \right]^{3/2} \left[ \frac{N_{eff}}{10^{16} cm^{-3}} \right]^{-3/4} \quad (26)$$

Where  $E_g$ ,  $N_{eff}$  are the band gap energy of silicon, and the effective doping concentration respectively. Furthermore, defects generated during irradiation cause changes in the effective doping concentration which are macroscopically modeled as a function of the radiation particle fluence,  $\Phi$  given by [25].

$$N_{eff} = 1.53 \times 10^{15} \exp[-1.139 \times 10^{-15} \Phi] \quad (27)$$

Avalanche parameters of a photodiode at a given operating voltage (at the fixed  $\lambda$  and  $T$ ) determine about a signal to noise ratio, a noise equivalent power (NEP) and resulting from it detectivity  $D$  or  $D^*$ . In correctly processed photodiode structures, their noise is of shot nature. The dependencies of total noise and dark noise on gain are [11].

$$I_N = [(2q[I_{ph} + I_{DB}]M^2 F(M) + I_{DS})B]^{1/2} \quad (28)$$

Substituting from equations (2), and (4) in to equation (28). The following equation can be obtained

$$I_N = [(2q\alpha\Phi MF(M) + I_{DS})B]^{1/2} \quad (29)$$

Where  $B$  is the system bandwidth. Moreover based on equation (9) the noise equivalent power can be calculated as follows [11]. The amount of optical power incident on the surface of a photodetector that produces a signal at the output of the detector just equal to the noise generated internally by the detector is the noise equivalent power (NEP). This is usually the minimum detectable signal level. On the other hand when we compare the detectors in terms of their detecting ability, the best detector is the one with the lowest NEP.

$$NEP = \frac{I_N / \sqrt{B}}{S_0 M} \quad (30) \quad (22)$$

However noise equivalent power (NEP) cannot be used as the only measure of a detector's relative performance, but rather detector detectivity at a specific wavelength and bandwidth should be used to determine the optimum detector type for a given application, so if we take the reciprocal of the NEP, we can define the detectivity. The higher the value of the detectivity, the better the detector. The detectivity ( $D$ ) is [23]

$$D = \frac{S_0 M}{I_N / B^{1/2}} = \frac{1}{NEP} \quad (31)$$

given by the following equation [8].

Nevertheless the NEP and hence the value of detectivity depends on the area of the detector. This makes it difficult to compare the intrinsic properties of two different types of detectors. To remove this dependence, we use another term, called  $D^*$  (detectivity normalized to the unit of detector area  $1 \text{ cm}^2$ ) to rate photodetectors.  $D^*$  is given by [11].

$$D^* = \frac{S_0 M A_d}{I_N / B^{1/2}} = \frac{A_d}{NEP} \quad (32)$$

### III. SIMULATION RESULTS AND DISCUSSIONS

We illuminate the effect of those environments on the optical signal detecting by APDs and how we can reduce the neutron effect in those devices. The results showed that the key to reducing thermal radiation effect is minimizing the active device volume and increasing device initial sensitivity or by selecting the materials that have lower ionization ratio. Moreover reducing the frequency band will contribute in improving detectivity and noise equivalent power. Furthermore optimizations of the device fabrication processes have resulted in significantly better electrical characteristics while maintaining good optical properties. The values of the parameters are shown in Table 1.

Table 1. List of the operating parameters used in model [1, 11, 24, 25]

Symbol	Operating parameter	Value
$\Phi$	Radiation Fluence	$1 \times 10^{11} \text{ n/cm}^2 - 5 \times 10^{12} \text{ n/cm}^2$
$T$	Ambient Temperature	300 K - 400 K
$P$	Incident Power	1 nW - 10 nW
$B$	Bandwidth	1 MHz - 2 MHz
$\lambda$	Incidence light Wavelength	800 nm - 1100 nm
$S_0$	Detector Initial Sensitivity	0.5 A/W - 0.75 A/W
$E_g$	Energy gap of Silicon	1.15 eV
$v$	Detector Volume	$2.5 \times 10^{-5} \text{ cm}^3 - 7.0 \times 10^{-5} \text{ cm}^3$
$k$	Boltzman's Constant	$1.38 \times 10^{-23} \text{ J/K}$
$R_L$	Load Resistance	4 K $\Omega$ - 5 K $\Omega$

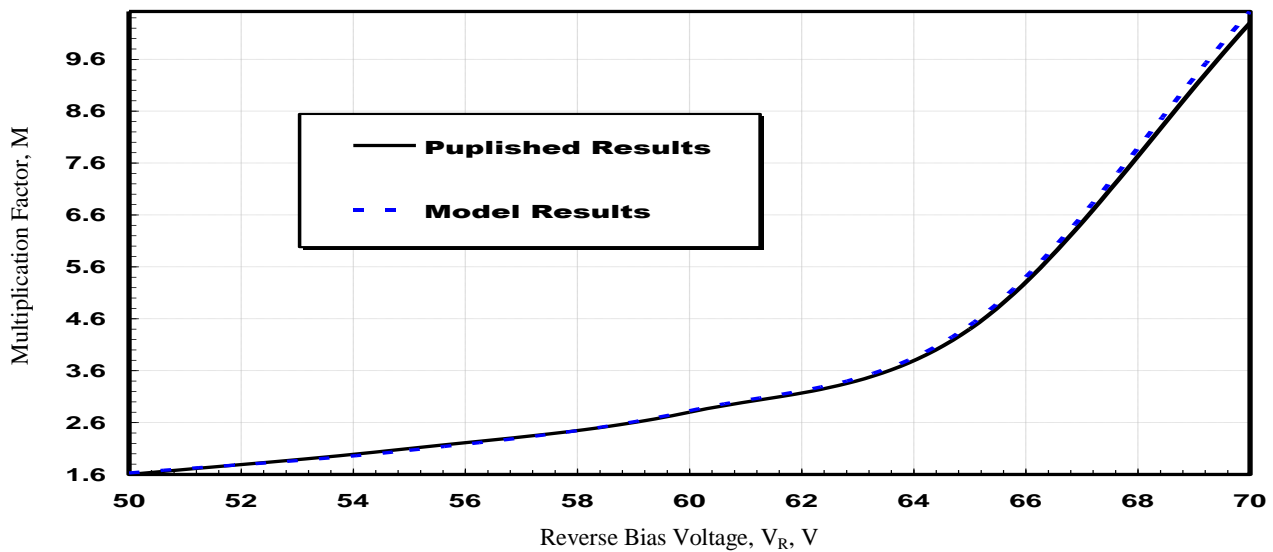


Fig.1. Variations of the multiplication factor ( $M$ ) against reverse bias voltage ( $V_R$ ) with  $T=300\text{K}$ ,  $P=10\text{nW}$ ,  $B=1\text{MHz}$ ,  $\Phi=1 \times 10^{11} \text{ n/cm}^2$ ,  $\lambda=850\text{nm}$ , and  $R_L=4.5 \text{ K}\Omega$ .

In figure (1) the typical computed values for the Multiplication Factor ( $M$ ) against reverse bias voltage ( $V_R$ ) under thermal effect, and experimental values are represented in the above figure that shows a good agreement between the resulted curve and published experimental curve.

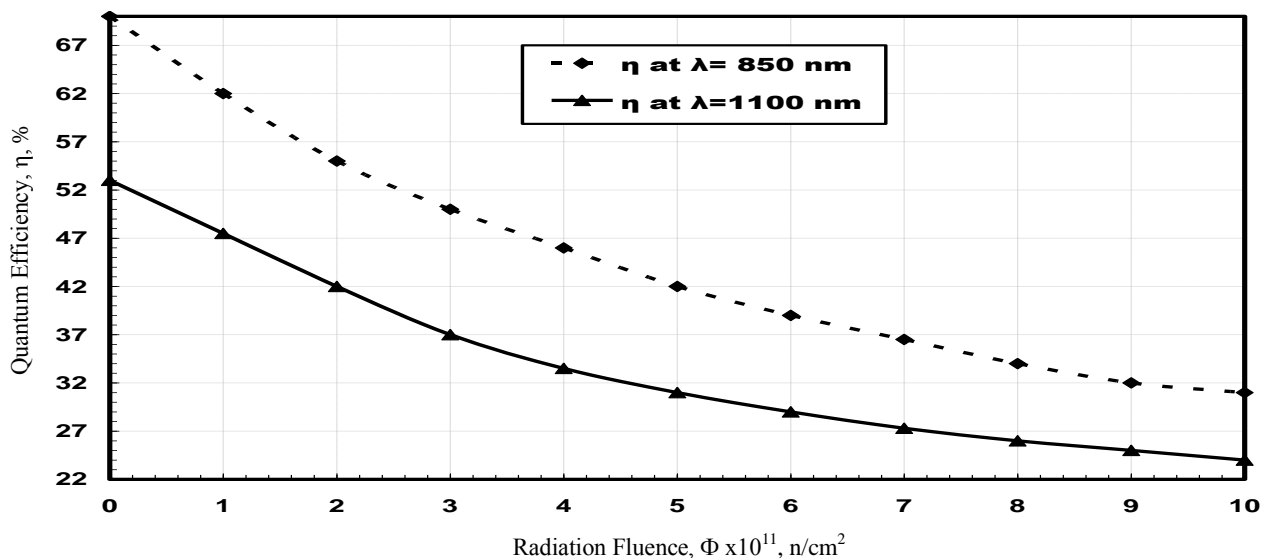


Fig.2. Variations of the quantum efficiency ( $\eta$ ) against radiation fluence ( $\Phi$ ) at different optical signal wavelength ( $\lambda$ ) with  $T=320\text{K}$ ,  $P=10\text{nW}$ ,  $B=1\text{MH}$ , and  $R_L=4 \text{ K}\Omega$ .

Figure (2) reveals the relation between quantum efficiency and radiation fluence at different incidence light wavelength. The figure illustrates that as the radiation fluence increases the device quantum efficiency is decreases. This can be explained by the fact that if the energy of neutron irradiation is high enough (above several hundred keV) the pair generation occurs. The energy spectrum of the energetic electrons is called "slowing spectrum". The energetic electron interacts with a lattice atom. As a result, the lattice atom is displaced from lattice site. This is so called Primary Knock on Atom (PKA). Interstitial (PKA), vacancy, and complex of them form a deep level in bandgap. This is so-called the generation-recombination centre [7]. Moreover these defects created throughout the optically active volume tend to decrease the overall collection efficiency of optically generated minority

carriers by reducing the minority carrier diffusion length [5]. Consequently the photocurrent decrease and hence, the device quantum efficiency decreases. In addition quantum efficiency decreases with increase incidence light wavelength. This can be explained by examining some basic material properties and the photocurrent generation mechanism. For indirect bandgap semiconductors, such as silicon, the optical absorption coefficient is usually relatively small for photons with energies only slightly larger than the material bandgap. This results in the creation of infrared (0.8  $\mu\text{m}$  - 1.1  $\mu\text{m}$  for Si) generated minority carriers farthest from the front optical surface and usually farthest from the electrical junction [5].



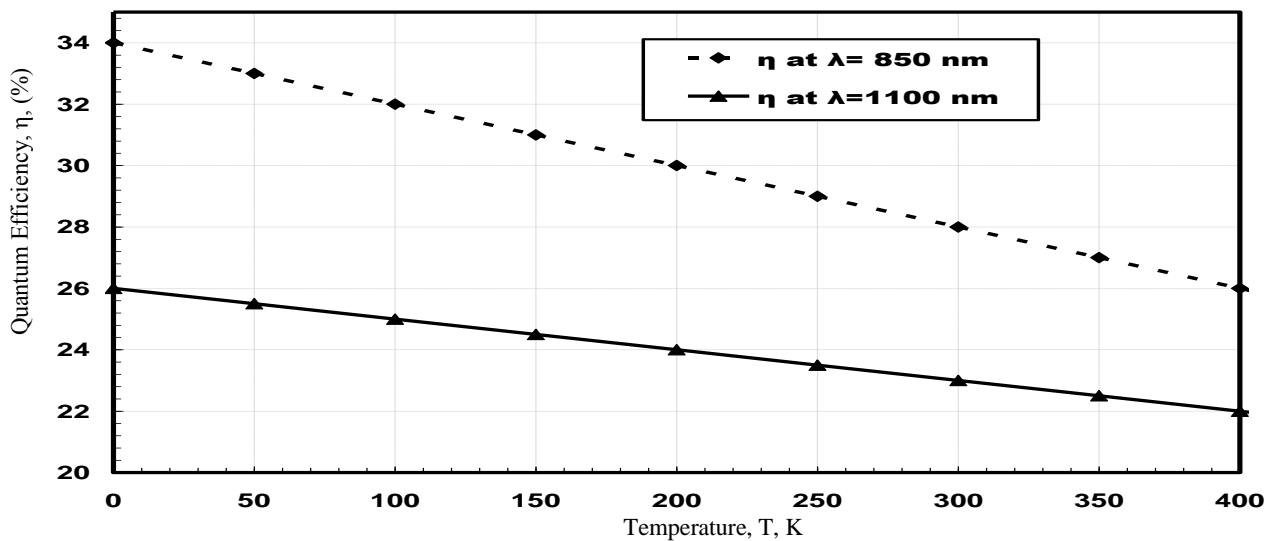


Fig.3. Variations of the quantum efficiency ( $\eta$ ) against temperature ( $T$ ) at different optical signal wavelength ( $\lambda$ ) with  $\Phi = 1 \times 10^{11}$  ( $n/cm^2$ ),  $P=10nW$ ,  $B=1MHz$ , and  $R_L=4 K\Omega$ .

Figure (3) reveals the relation between quantum efficiency and temperature at different incidence light wavelength. The figure shows that as the temperature increases the device quantum efficiency decreases. This can be attributed to the fact that temperature plays a significant role in the number of reactions that take place during/after irradiation as a rise in  $10^0C$  can double the reaction rates [26]. Therefore this duplication of defects created throughout the optically active

volume tends to decrease the overall collection efficiency of optically generated minority carriers by reducing the minority carrier diffusion length [5]. This is the reason of why dark current increases by a double of its value for each rise in temperature of  $10^0C$  [24]. In addition, the avalanche process statistics generate current fluctuations these fluctuations increases with the temperature, and APD efficiency degraded [8].

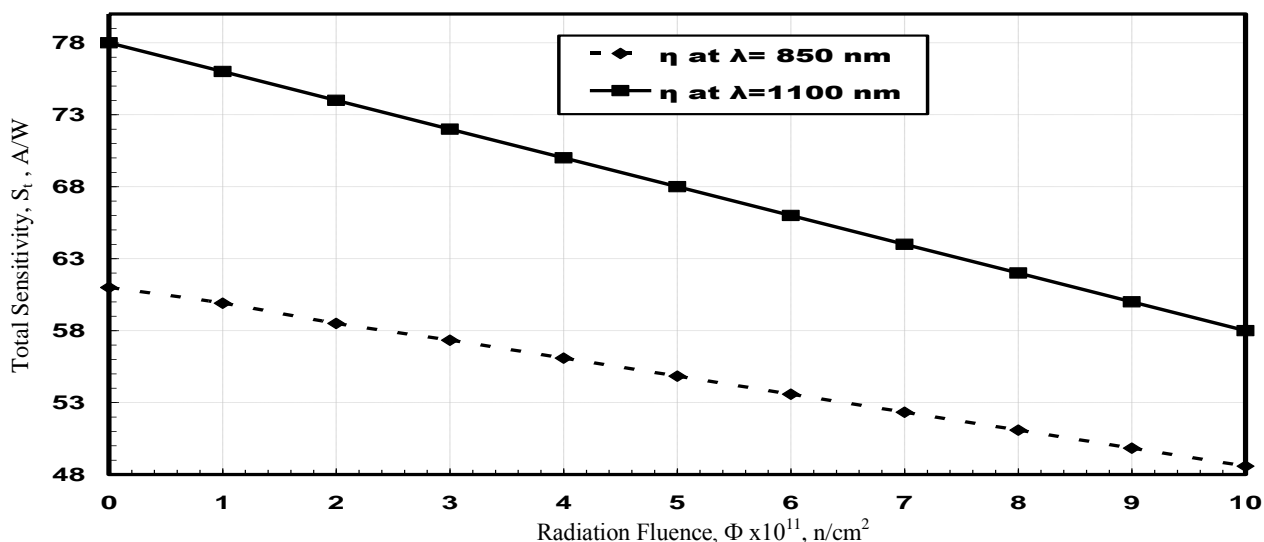


Fig. 4. Variations of the total sensitivity ( $S_t$ ) against radiation fluence ( $\Phi$ ) at different optical signal wavelength ( $\lambda$ ) with  $T=320K$ ,  $P=10nW$ ,  $B=1MHz$ , and  $R_L=4 K\Omega$ .

Figure (4) reveals the relation between total sensitivity and radiation fluence. It shows the reduction in optical sensitivity with increasing neutron radiation. This is because radiation induced defects created throughout the optically active volume tending to decrease the overall collection of optically generated minority carriers by reducing the minority carrier diffusion length. The crystal damage clusters serve as recombination sites causing optically generated hole-electron pairs to recombine before they can

contribute to junction current [5]. In addition sensitivity is limited by photon shot noise which increases with increase dark current in the radiation field [8]. Moreover the shorter the wavelength of incident radiation is the higher noise current  $I_N$  and lower the gain  $M$  for  $I_N = \text{const}$ . Worsening of photodiode properties for shorter wavelengths results from the increase of number of holes participating in total current flowing through the avalanche region. Therefore from

equation (20) this will reduce total sensitivity at shorter wavelengths [7].

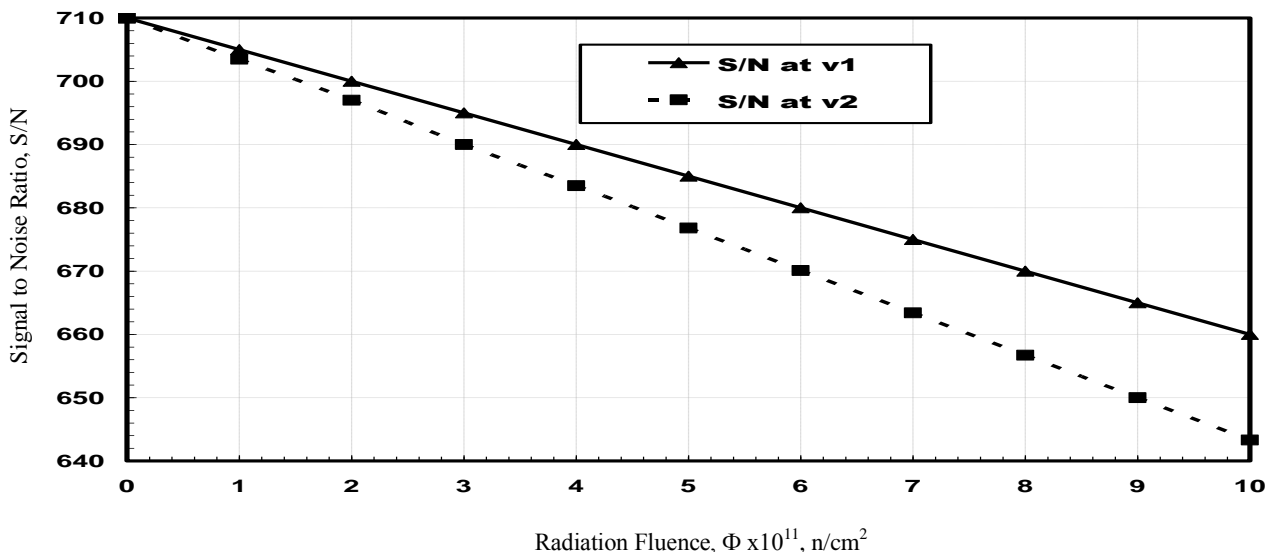


Fig.5. Variations of the signal to noise ratio (S/N) against radiation fluence ( $\Phi$ ) at different active volume ( $v$ ) where ( $v_1 = 2.4 \times 10^{-5}$  cm<sup>3</sup>,  $v_2 = 7 \times 10^{-5}$  cm<sup>3</sup>) with  $T=320$ K,  $P=10$ nW,  $B=1$ MHz, and  $R_L=4$  K $\Omega$ .

Figure (5) reveals the relation between signal to noise ratio and radiation fluence. The instantaneous photocurrent generated in photodiodes during exposure to a pulse of ionizing radiation is a result of a combination of Compton scattering effects and the photoelectric effect, depending on the energy of the ionizing-radiation photon. Both mechanisms create excited electrons which generate many electron-hole pairs as the excited electrons move through the crystal lattice. These electron-hole pairs can contribute to the device current if they are created within approximately one diffusion length of the semiconductor depletion region edge. This ionizing-radiation induced photocurrent can be significantly larger than the intended signal current

component, depending on the amplitude of the ionizing-radiation field and the amplitude of the signal intensity. Moreover an increase in the photodiode dark (leakage) current results in a larger background noise level. Consequently the signal to noise ratio decrease. However by minimizing the active device volume, the magnitude of the radiation induced signal current can be reduced. Relatively short minority carrier diffusion lengths also decrease the number of ionizing-radiation induced minority carriers that contribute to the device current [5]. Small active volume photodiode structures are used to achieve low noise current generation during exposure to ionizing-radiation and as a result increase the signal to noise ratio [6].

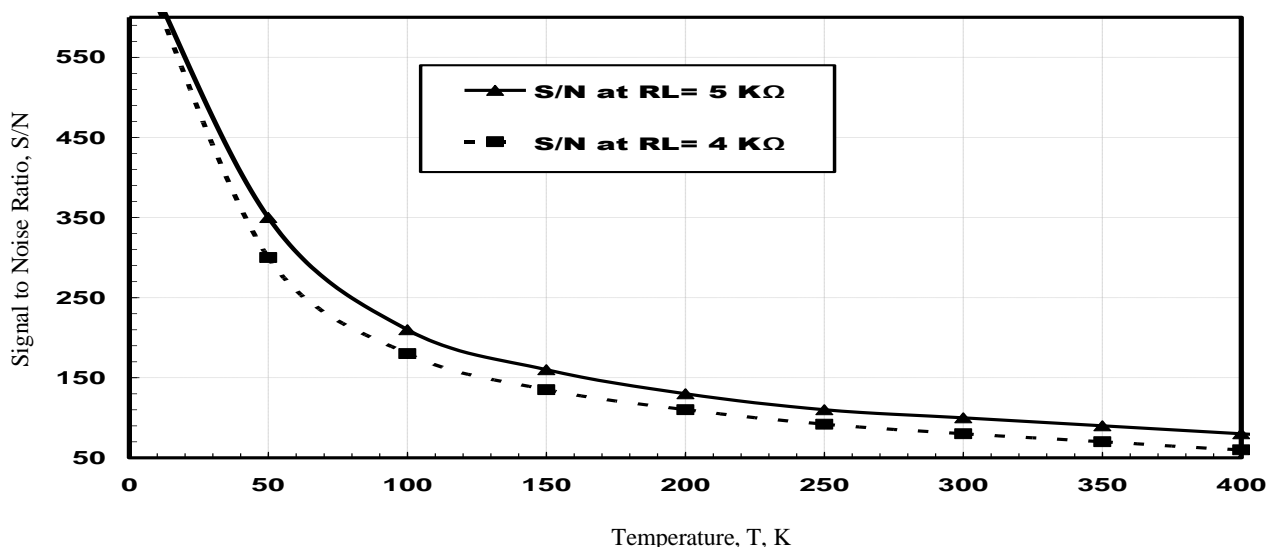


Fig.6. Variations of the signal to noise ratio (S/N) against temperature (T) at different load resistance ( $R_L$ ) with  $\Phi = 1 \times 10^{11}$  (n/cm<sup>2</sup>),  $P=10$ nW,  $B=1$ MHz, and  $R_L=4$  K $\Omega$ .

Figure (6) reveals the relation between signal to noise ratio and temperature at different load resistance. From the figure

signal to noise ratio decreases as temperature increase. This can be attributed to the fact that temperature plays a

significant role in the number of reactions that take place during/after irradiation as a rise in  $10^0\text{C}$  can double the reaction rates [26]. Therefore this duplication of defects created throughout the optically active volume tends to increase photodiode dark current and therefore photodiode noise power level [5]. So the signal to noise ratio decrease

with temperature. Moreover for the higher values of a load resistance the value of thermal noise decreases. Hence, the value of signal to noise ratio increase. Therefore in order to have maximal value of a signal to noise ratio the high values of load resistance should be taken [24].

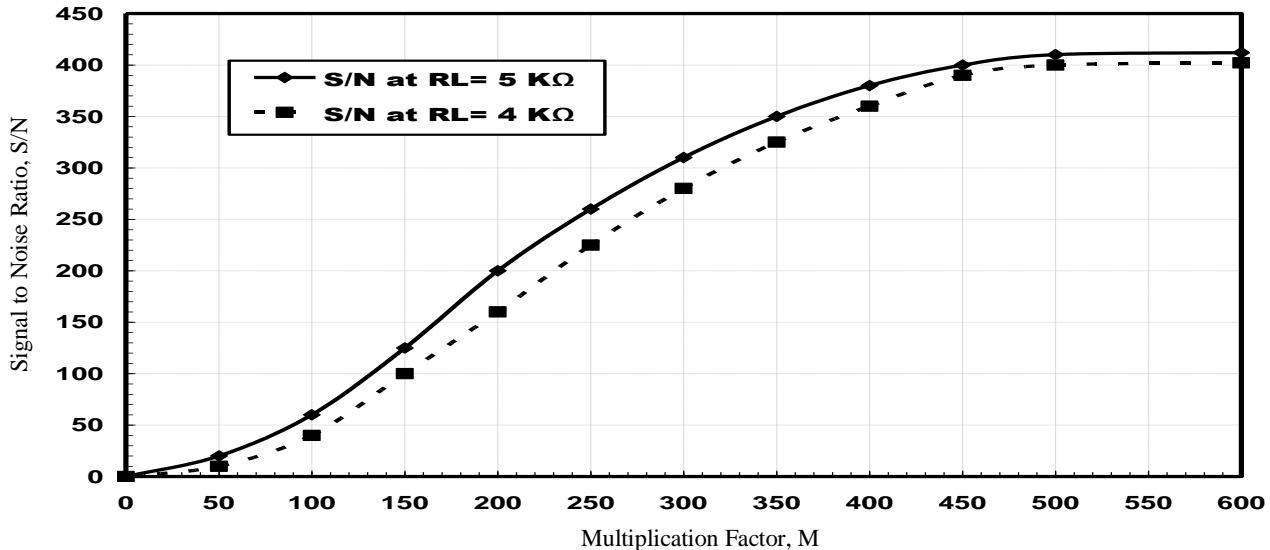


Fig.7. Variations of the signal to noise ratio (S/N) against multiplication factor (M) at different load resistance ( $R_L$ ) with  $\Phi = 1 \times 10^{11}$  ( $\text{n}/\text{cm}^2$ ),  $P=10\text{nW}$ ,  $T=320\text{ K}$ ,  $B=1\text{MHz}$ , and  $R_L=4\text{ K}\Omega$ .

Figure (7) reveals the relation between signal to noise ratio and multiplication factor at different load resistance. From the figure signal to noise ratio increases as multiplication factor increase. This can be attributed to the fact that a mechanism of internal gain causes significant increases in a signal current generated in a detector and improves the

signal to noise ratio. Such a mechanism, however dose not influence on the noises originated from a load resistance as will as the amplifier noises [24]. Furthermore as thermal noises decreases with increase the load resistance this will contribute in increasing the signal to noise ratio of avalanche photodiode.

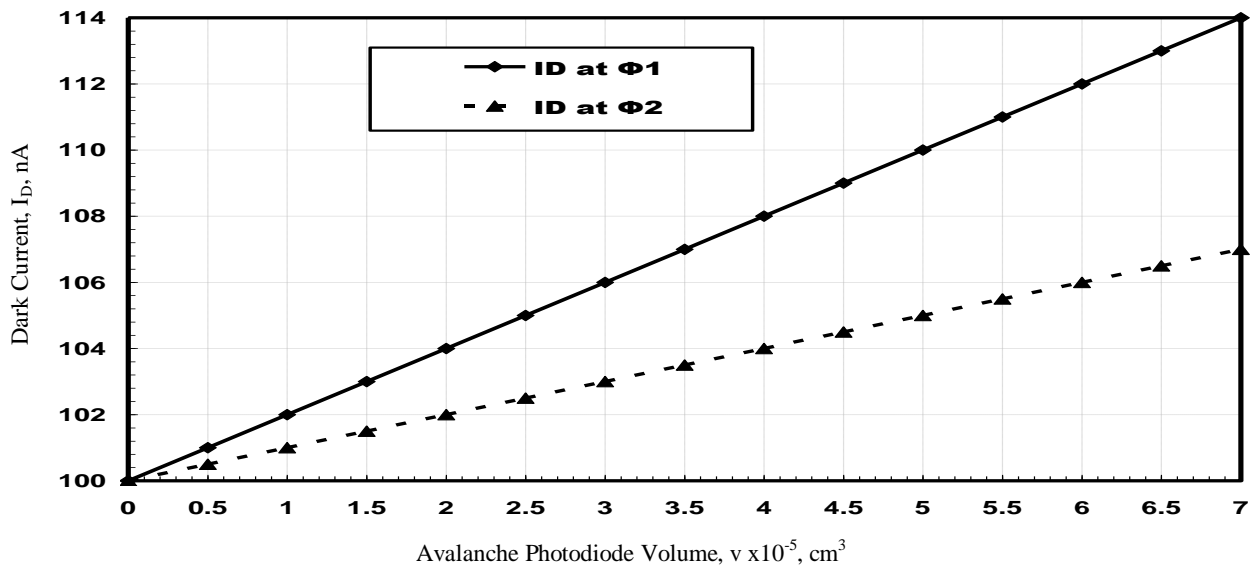


Fig.8. Variations of the dark current ( $I_D$ ) against avalanche photodiode volume ( $v$ ) at different radiation fluencies where ( $\Phi_1=2 \times 10^{11} \text{ n}/\text{cm}^2$ ,  $\Phi_2=1 \times 10^{11} \text{ n}/\text{cm}^2$ ) ( $\Phi$ ) with  $T=320\text{K}$ ,  $P=10\text{nW}$ ,  $B=1\text{MHz}$ , and  $\lambda=850\text{nm}$ .

Figure (8) reveals the relation between the dark current ( $I_D$ ) and the device volume ( $v$ ); from the figure it is apparent that the dark current increase as the device volume increase. Moreover the induced dark current is increases as the neutron fluence increase. This result can be attributed to the creation of the defects in the silicon lattice which are responsible for the increase of the dark current is a volume

effect, so usually the using of APD that has large volume will contribute in increasing of dark current  $I_D$  increment than APD that has small device volume. Moreover by minimizing the active device volume, the magnitude of the radiation induced signal current can be reduced. Relatively short minority carrier diffusion lengths also decrease the number of ionizing-radiation induced minority carriers that

contribute to the device current [5]. Furthermore Care must be taken not to make the active region thickness too narrow or the minority carrier diffusion length too small or the desired optically generated minority carriers will not contribute to the device current and the optical responsivity will be suboptimal [5].

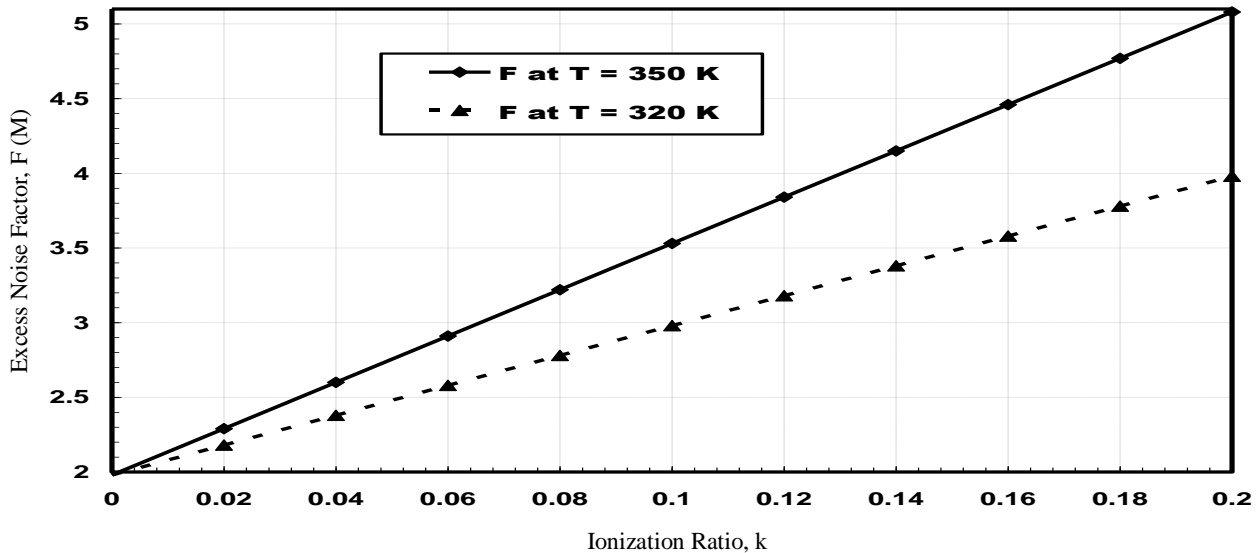


Fig.9. Variations of the excess noise factor (F) against ionization ratio (k) at different temperatures (T) with  $P=10\text{nW}$ ,  $B=1\text{MHz}$ ,  $\Phi=1 \times 10^{11} \text{ n/cm}^2$ ,  $\lambda=850\text{nm}$ , and  $R_L=4 \text{ K}\Omega$ .

Figure (9) reveals the relation between the excess noise factor  $F$  (M) and the ionization ratio ( $k$ ); from the figure it is apparent that the excess noise factor increase with increasing the temperature and ionization ratio. This result can be attributed to; all avalanche photodiodes generate excess noise due to the statistical nature of the avalanche process [8]. In addition these avalanche process statistics generate current fluctuations these fluctuations increases

with the temperature, and APD performance is degraded by an excess noise factor ( $F$ ) compared to a PIN especially at higher temperatures [8]. Furthermore the excess noise factor is a function of the carrier ionization ratio,  $k$ , where  $k$  is usually defined as the ratio of hole to electron ionization probabilities [8]. Therefore the lower the values of  $k$  the lower the excess noise factor [8].

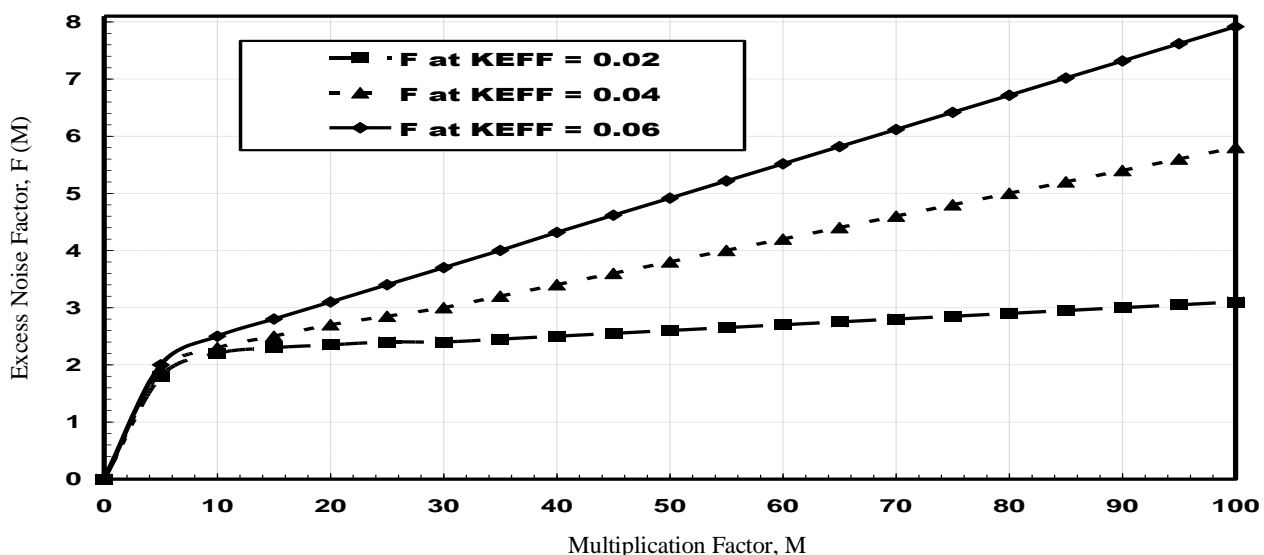


Fig.10. Variations of the excess noise factor (F) against multiplication factor (M) at different effective k-factor with  $T=320\text{K}$ ,  $P=10\text{nW}$ ,  $B=1\text{MHz}$ ,  $\Phi=1 \times 10^{11} \text{ n/cm}^2$ ,  $\lambda=850\text{nm}$ , and  $R_L=4 \text{ K}\Omega$ .

Figure (10) reveals the relation between the excess noise factor  $F$  (M) and the multiplication factor ( $M$ ); from the figure it is apparent that the excess noise factor increase with increasing multiplication factor. This result can be accredited to the fact that all avalanche photodiodes

generate excess noise due to the statistical nature of the avalanche process [8]. Therefore, higher multiplication factor results in higher excess noise factor. Moreover the excess noise factor is a function of the carrier ionization ratio,  $k$ , where  $k$  is usually defined as the ratio of hole to



electron ionization probabilities [8]. Therefore the lower the values of  $k$  and  $M$ ; the lower the excess noise factor [8].

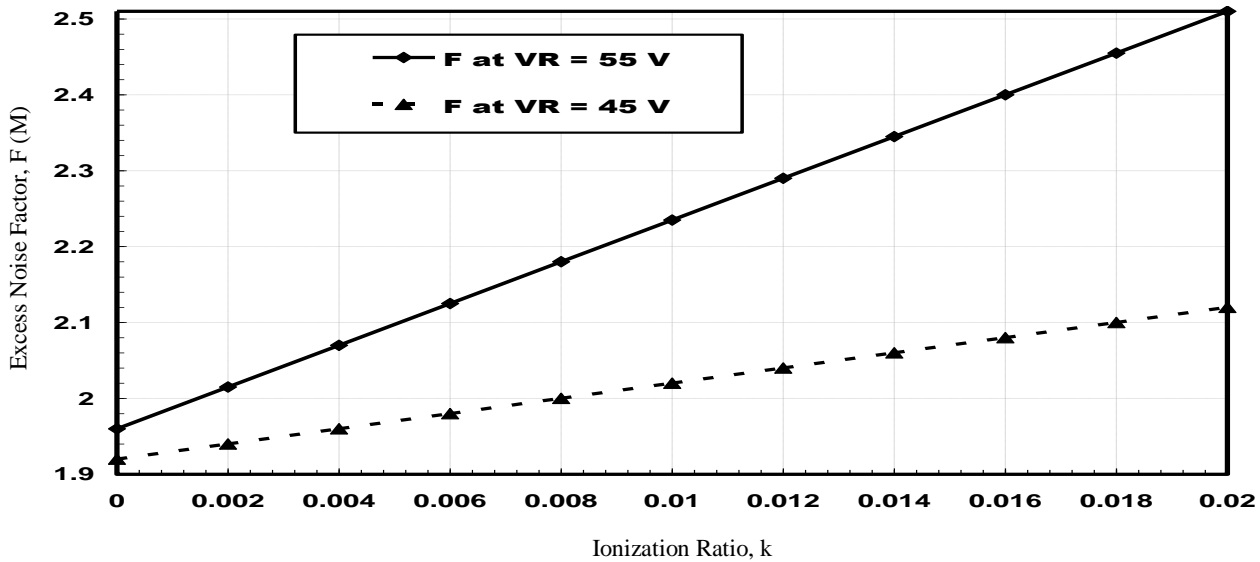


Fig.11. Variations of the excess noise factor (F) against ionization ratio ( $k$ ) at different reverse bias voltage ( $V_R$ ) with  $T=320K$ ,  $P=10nW$ ,  $B=1MHz$ ,  $\Phi=1 \times 10^{11} n/cm^2$ ,  $\lambda=850nm$ , and  $R_L=4 K\Omega$ .

Figure (11) reveals the relation between the excess noise factor  $F$  ( $M$ ) and the ionization ratio ( $k$ ) at different reverse bias voltage; from the figure the excess noise factor increase with increasing reverse voltage. This result can be credited

to higher reverse bias voltage results in higher multiplication factor [24]. However the avalanche gain causes an increase in excess noise. Therefore the excess noise factor increases with increase reverses bias voltage.

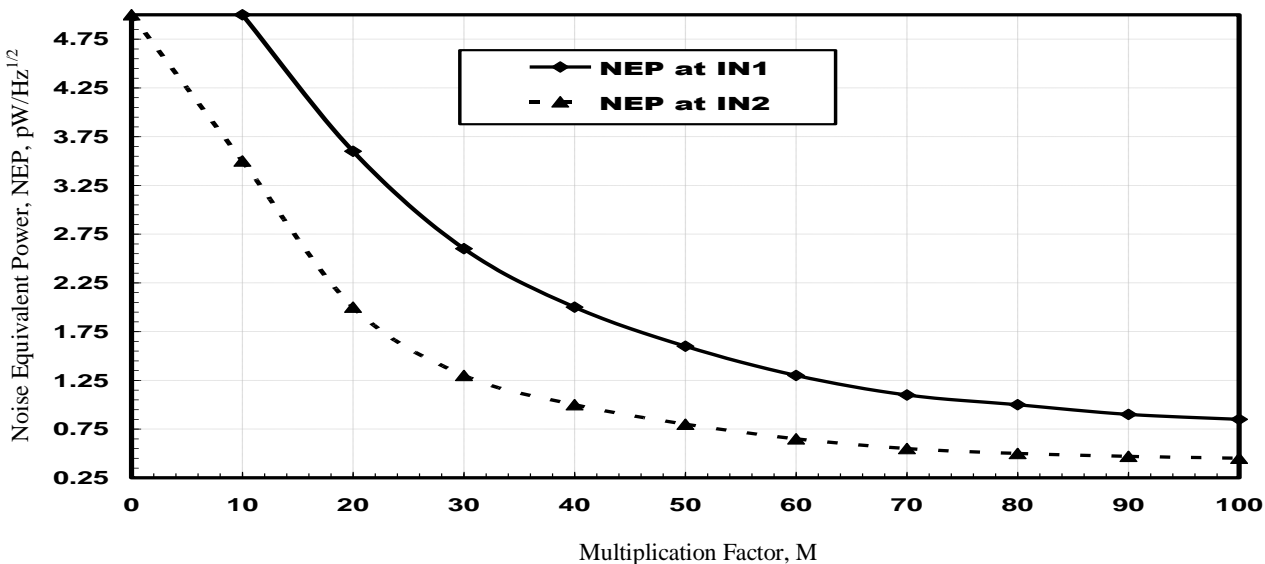


Fig.12. Variations of the noise equivalent power (NEP) against multiplication factor ( $M$ ) at different Noise current ( $I_N$ ) where ( $I_{N1}= 0.4 pA/Hz^{1/2}$ ,  $I_{N2}= 0.2 pA/Hz^{1/2}$ ) with  $T=320K$ ,  $P=10nW$ ,  $B=1MHz$ ,  $\Phi=1 \times 10^{11} n/cm^2$ ,  $\lambda=850nm$ , and  $R_L=4 K\Omega$ .

Figure (12) reveals the relation between noise equivalent power and the multiplication factor. In addition based on the definition of NEP that is the amount of optical power incident on the surface of a photodetector that produces a signal at the output of the detector just equal to the noise generated internally by the detector. This is usually the

minimum detectable signal level. On the other hand a mechanism of internal gain causes significant increases in a signal current generated in a detector and improves the signal to noise ratio [24]. So that NEP reduces with increasing the multiplication factor. Furthermore in figure (7) since noise currents which proportional to the square

root of leakage currents determine the minimum detection levels [24]. Therefore NEP value decreases with lower noise current.

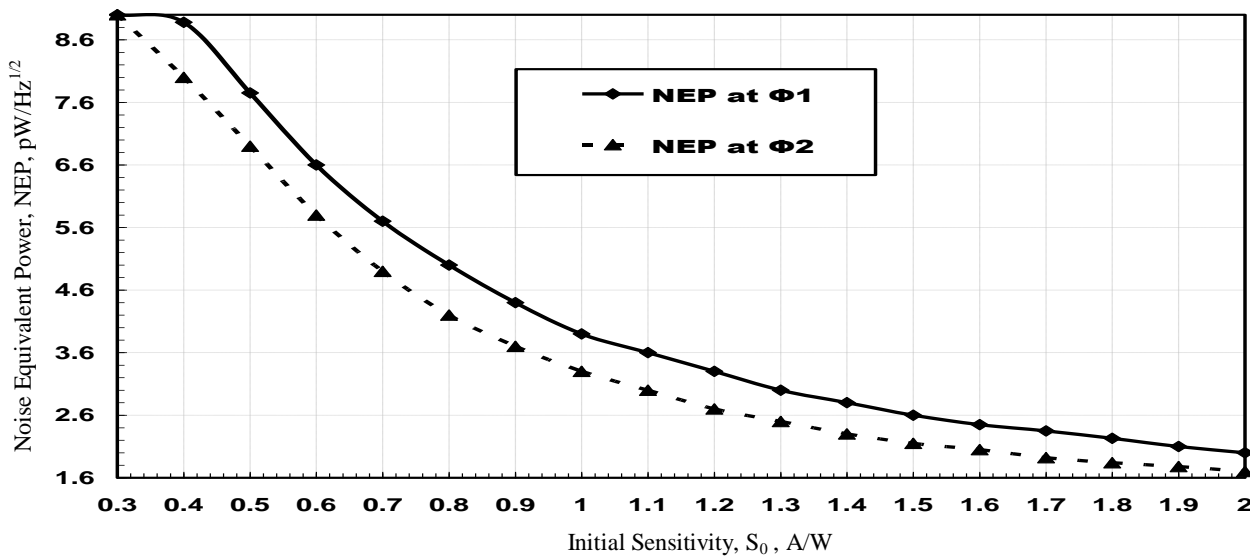


Fig.13. Variations of the noise equivalent power (NEP) against initial sensitivity ( $S_0$ ) at different radiation fluencies ( $\Phi$ ) where ( $\Phi_1=5 \times 10^{12}$  n/cm<sup>2</sup>,  $\Phi_2=1 \times 10^{11}$  n/cm<sup>2</sup>) with  $P=10$ nW,  $B=1$ MHz,  $T=320$ K,  $\lambda=850$ nm, and  $R_L=4$  K $\Omega$ .

Figure (13) reveals the relation between the noise equivalent power (NEP) and the Initial sensitivity ( $S_0$ ) at different radiation fluencies, from the figure, noise equivalent power decrease with increasing device initial sensitivity, since NEP represents the minimum detectable signal level. However neutron irradiation is believed to cause large clusters of disorder in the crystal lattice due to the relatively large energy transfer associated with neutron scattering. These

disorder clusters in the crystal lattice create generation sites in the depletion region of the semiconductor junction. This causes an increase in the depletion layer generation recombination current. This results in an increase in the photodiode dark (leakage) current and therefore a larger background noise level [5]. Furthermore this tends to raise the minimum power level of detectable optical signals. So this leads to NEP increment [6].

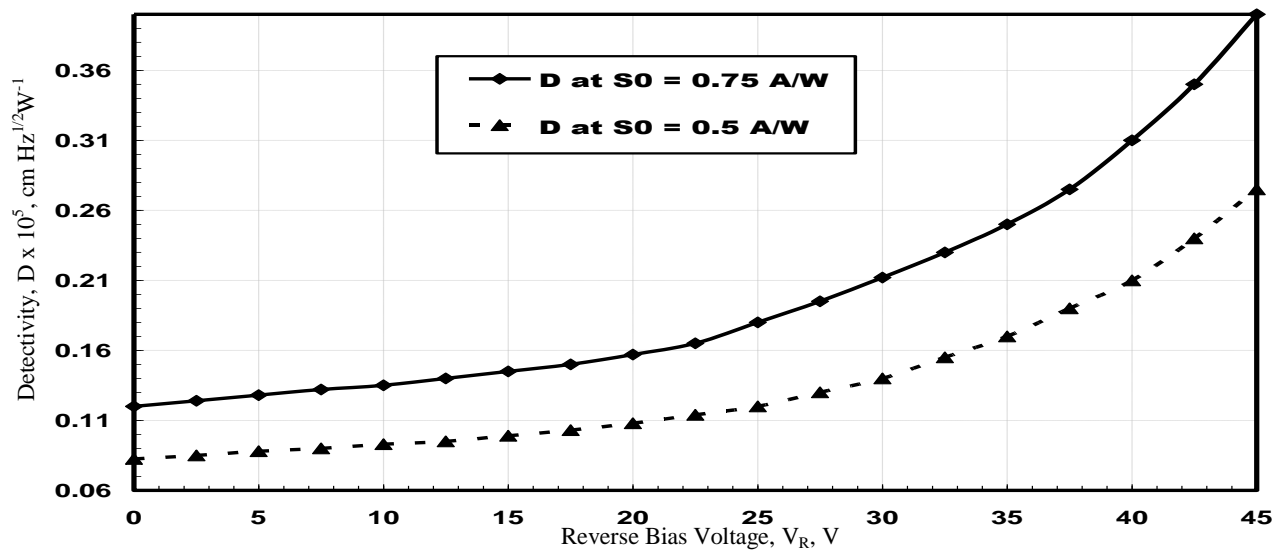


Fig.14. Variations of the detectivity (D) against reverse bias voltage ( $V_R$ ) at different initial sensitivity ( $S_0$ ) with  $P=10$ nW,  $B=1$ MHz,  $\Phi=1 \times 10^{11}$  n/cm<sup>2</sup>,  $\lambda=850$ nm, and  $R_L=4$  K $\Omega$ .

Figure (14) reveals the relation between detectivity (D) and the Reverse bias voltage ( $V_R$ ) at different initial sensitivity ( $S_0$ ); from the figure it is apparent that the detectivity increase with increasing reverse bias voltage. For the reason

that reverse bias voltage results in increasing multiplication factor which causes significant increases in a signal current generated in a detector and improves the signal to noise ratio [24]. Furthermore this result in reducing the minimum

power level of detectable optical signals [20]. Consequently detectivity will increase.

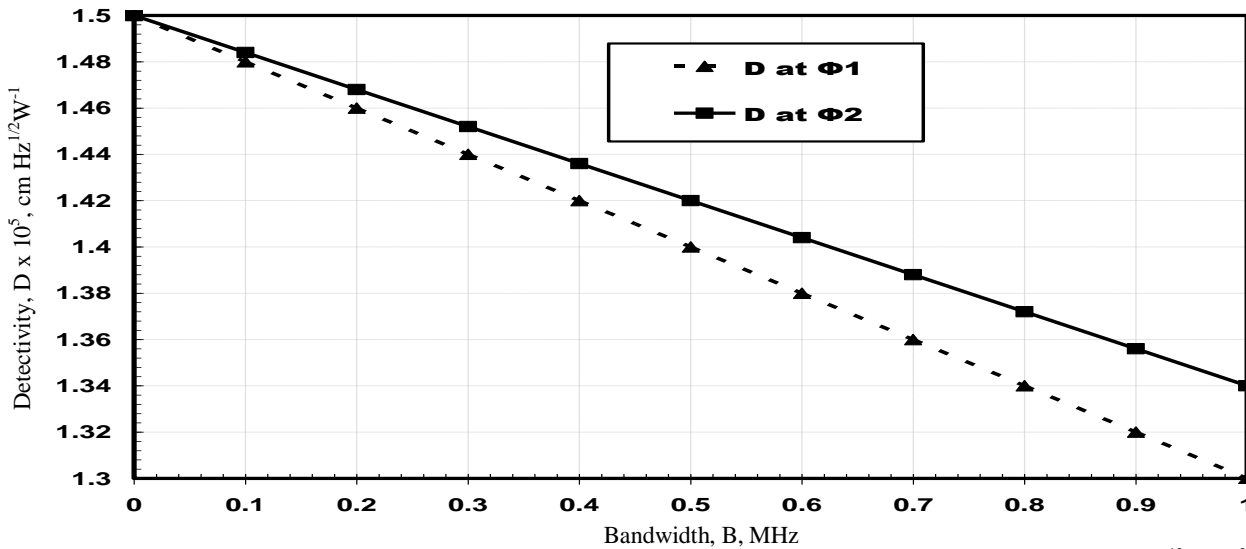


Fig.15. Variations of the detectivity (D) against bandwidth (B) at different radiation fluencies ( $\Phi$ ) where ( $\Phi_1= 5 \times 10^{12} \text{ n/cm}^2, \Phi_2= 1 \times 10^{11} \text{ n/cm}^2$ ) with  $P=10\text{nW}, T=320\text{K}, \Phi=1 \times 10^{11} \text{ n/cm}^2, \lambda=850\text{nm}$ , and  $R_L=4 \text{ K}\Omega$ .

Figure (15) reveals the relation between detectivity (D) and the bandwidth (B) at different radiation fluencies ( $\Phi$ ); from the figure it is apparent that the detectivity decrease with increasing bandwidth. This result can be endorsed to while impact ionization can increase the APDs detectivity it still limits their bandwidth at high M because of the long multiplication chains, which takes time to build up and die

away. This accompanying increase in response time with M results in a roughly constant gain bandwidth product [2]. While increasing the avalanche gain the detectivity increase it causes both, an increase in the noise originated from the dark current and in the quantum noise this restricts the bandwidth [24].

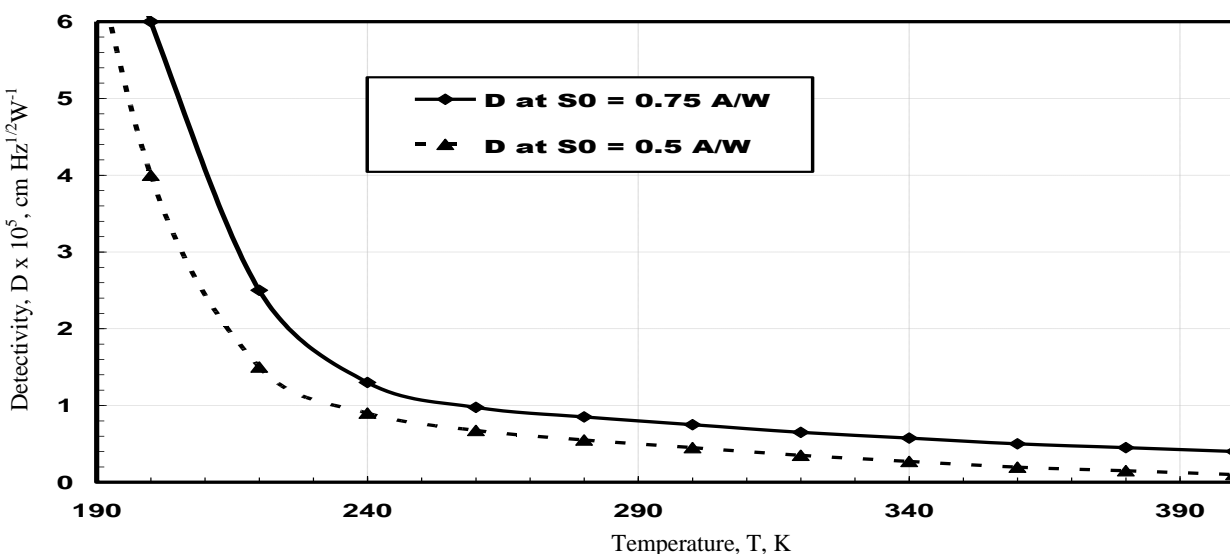


Fig.16. Variations of the detectivity (D) against temperature (T) at different initial sensitivity ( $S_0$ ) with  $P=10\text{nW}, B=1\text{MHz}, \Phi=1 \times 10^{11} \text{ n/cm}^2, \lambda=850\text{nm}$ , and  $R_L=4 \text{ K}\Omega$ .

Figure (16) reveals the relation between detectivity ( $D$ ) and the temperature ( $T$ ) at different initial sensitivity ( $S_0$ ); from the figure it is apparent that the detectivity decrease with increasing temperature. For the reason that rises in  $10^0\text{C}$  can double the reaction rates that take place during/after irradiation [26]. Therefore this duplication of defects created throughout the optically active volume tends to decrease the overall collection of optically generated minority carriers by reducing the minority carrier diffusion length and increase the dark current [5]. Moreover the avalanche process statistics generate current fluctuations these fluctuations

increases with the temperature [24]. As a result this will raise the minimum optical power an optical detector can sense and reduce device detectivity [5].

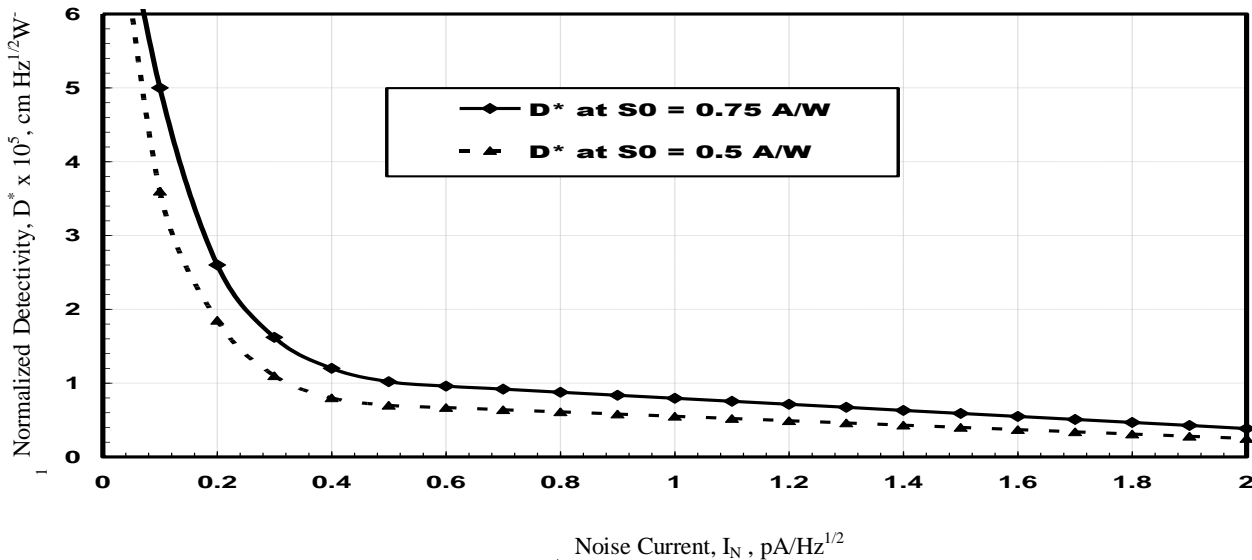


Fig.17. Variations of the normalized detectivity ( $D^*$ ) against noise current ( $I_N$ ) at different Initial sensitivity ( $S_0$ ) with  $T=320\text{K}$ ,  $P=10\text{nW}$ ,  $B=1\text{MHz}$ ,  $\Phi=1 \times 10^{11}$  n/cm<sup>2</sup>,  $\lambda=850\text{nm}$ , and  $R_L=4$  K $\Omega$ .

Figure (17) reveals the relation between normalized detectivity ( $D^*$ ) and the Noise current ( $I_N$ ); from the figure it is apparent that the normalized detectivity decrease with both increasing noise current and decrease the initial sensitivity. This result can be attributed to increasing the noise current will reduce signal to noise ratio and tends to impose a lower bound on the minimum detectable optical signal for a given signal to noise ratio [6]. Therefore higher noise current results in lower normalized

detectivity. Moreover decrease the initial sensitivity result in raising the minimum power level of detectable optical signals [20], hence the normalized detectivity decrease.

#### IV. CONCLUSION

In this paper a block diagram model treating the radiation induced damage is proposed to provide a mean to control the optical properties of APDs in thermal radiation environments. The proposed treatment can be used to improve the detectivity and noise equivalent power as well as the normalized detectivity. A model is built using VisSim environment. The obtained results showed that the key to reducing thermal radiation effect would expect in minimizing the active device volume. In the same time this provides higher detector sensitivity and responsivity as well as detector efficiency. Moreover increase signal to noise ratio can be achieved by increase the load resistance. Furthermore increasing reverse bias voltage results in increase avalanche gain multiplication factor. Moreover reducing the frequency band will contribute in improving detectivity and noise equivalent power. Furthermore this can be achieved by selecting the materials that have lower

ionization ratio through the fabrication process. These results are significant for many applications in which noise currents which proportional to the square root of leakage currents determine the minimum detection levels. The results are validated against published experimental work in temperature case and show good agreement.

#### V. REFERENCES

- [1] M. Kovacevic, S. Savovic, A. Djordjevich, J. Bajic, D. Stupar, M. Kovacevic, and S. Simic, "Measurements of growth and decay of radiation induced attenuation during the irradiation and recovery of plastic optical fibres", *Optics and Laser Technology*, Vol. 47, pp. 148–151, 2013.
- [2] C. Tan, J. Ng, S. Xie, and J. David, "Potential materials for avalanche photodiodes operating above 10Gb/s", *International Conference on Computers and Devices for Communication*, Vol. 9, pp. 152-157, 2009.
- [3] A. Kalma, and W. Hardwick, "Radiation testing of pin photodiodes", *IEEE Transaction on Nuclear Science*, Vol. 25, pp. 1483-1488, 1978.

- [4] S. M. Eladl, "Modeling of ionizing radiation effect on optoelectronic-integrated devices (OEIDs)", *Microelectronics Journal*, Vol. 40, pp.193–196, 2009.
- [5] J. Wiczer, T. Fischer, L. Dawson, G. Osbourn, T. Zipperian, and C. Barnes, "Pulsed irradiation of optimized, mbe grown, AlGaAs/GaAs radiation hardened photodiodes", *IEEE Transaction on Nuclear Science*, Vol. 31, pp. 1477-1482, 1984.
- [6] J. Wiczer, L. Dawson, G. Osbourn, and C. Barnes, "Permanent damage effects in si and AlGaAs/GaAs photodiodes", *IEEE Transaction on Nuclear Science*, Vol. 29, pp. 1539-1544, 1982.
- [7] D. Nikolic, A. Vasic, I. Fetahovic, K. Stankovic, and P. Osmokrovic, "Photodiode Behavior in Radiation Environment", *Application Mathematics Information and Mechanics*, Vol. 3, pp. 27-34, 2011.
- [8] *Avalanche Photodiodes: A User's Guide*, PerkinElmer, 2003.
- [9] M. C. Teich, K. Matsuo, and B. E. A. Saleh, "Counting distributions and error probabilities for optical receivers incorporating superlattice avalanche photodiodes", *IEEE Transactions on Electron Devices*, Vol. 33, pp. 1475-1488, 1986.
- [10] J. S. Laird, S. Onoda, T. Hirao, L. Edmonds, and T. Ohshima, "Quenching of impact ionization in heavy ion induced tracks in wide bandwidth si avalanche photodiodes", *IEEE Transaction on Nuclear Science*, Vol. 9, pp. 1704-1709, 2007.
- [11] I. Wegrzecka, M. Wegrzecki, M. Grynglas, J. Bar, A. Uszynski, R. Grodecki, P. Grabiec, S. Krzeminski, and T. Budzynski, "Design and properties of silicon avalanche photodiodes", *Opto-Electronics Review*, Vol. 12, pp. 95–104, 2004.
- [12] J. S. Laird, T. Hirao, S. Onoda, H. Ohyama, and T. Kamiya, "Heavy-ion induced single-event transients in high-speed InP-InGaAs avalanche photodiodes", *IEEE Transaction on Nuclear Science*, Vol. 50, pp. 2225-2232, 2003.
- [13] R. H. West, "A local view of radiation effects in fiber optics", *Journal of Lightwave Technology*, Vol. 6, pp. 155-164, 1988.
- [14] S. Baccaro, J. Bateman, F. Cavallari, V. Ponte, K. Deiters, P. Denes, M. Diemoz, T. Kirn, A. Lintern, E. Longo, M. Montecchi, Y. Moussienko, J. Pansart, D. Renker, S. Reucroft, G. Rosi, R. Rusack, D. Ruuska, R. Stephenson, and M.J. Torbet, "Radiation damage effect on avalanche photodiodes", *CMS Conference*, Vol. 10, pp. 1-7, 1998.
- [15] H. Lischka, H. Henschel, W. Lennartz, and H. U. Schmidt, "Radiation sensitivity of light emitting diodes (LED), laser diodes (LD) and photodiodes (PD)", *IEEE Transaction on Nuclear Science*, Vol. 91, pp. 404-408, 1992.
- [16] A. Niemela, H. Sipila, and V.I. Ivanov, "High-resolution p-i-n CdTe and CdZnTe X-Ray detectors with cooling and rise-time discrimination", *IEEE Transactions on Electron Devices*, Vol. 30, pp. 549-553, 1996.
- [17] S. Onoda, T. Hirao, J. S. Laird, T. Wakasa, T. Yamakawa, T. Okamoto, Y. Koizumi, and T. Kamiya, "Development of monte-carlo modeling for proton induced charge in si pin photodiode", *IEEE Transaction on Nuclear Science*, Vol. 51, pp. 2770-2775, 2004.
- [18] L. Shi, S. N. Nihtianov, F. Scholze, and L. K. Nanver, "Electrical performance stability characterization of high-sensitivity si-based EUV photodiodes in a harsh industrial application", *IEEE Transaction on Nuclear Science*, Vol. 2, pp. 3952-3957, 2012.
- [19] T. English, G. Malley, and R. Korde, "Neutron hardness of photodiodes for use in passive rubidium frequency standards", *IEEE Annual Frequency Control Symposium*, Vol. 2, pp. 532-539, 1988.
- [20] K. Gill, V. A. Engels, J. Batten, G. Cervelli, R. Grabit, C. Mommaert, G. Stefanini, J. Troska, and F. Vasey, "Radiation Damage Studies of Optoelectronic Components for the CMS Tracker Optical Links", *IEEE Transaction on Nuclear Science*, Vol. 98, pp. 405-412, 1998.
- [21] J. Jiménez, J. S. Páramo, M. Álvarez, J. Domínguez, J. Oter, I. Arruego, R. Tamayo, and H. Guerrero, "Proton radiation effects on medium/large area Si PIN photodiodes for Optical Wireless Links for Intra-Satellite Communications (OWLS)", *IEEE Transaction on Nuclear Science*, Vol. 7, pp. 73-79, 2007.
- [22] Ahmed Nabih Zaki Rashed, "Performance Response Characteristics of Avalanche Photodiodes (APDs) Under High Thermal and Protons Irradiation Environments", *Global Advanced Research Journal of Engineering, Technology and Innovation*, Vol. 1, pp. 033-042, 2012.
- [23] Z. SU, and X. Liang, "Computation and analysis on The volt-ampere characteristics of photodiode sensor under the certain conditions", *IEEE International Congress on Image and Signal Processing*, Vol. 7, pp. 2593-2596, 2011.
- [24] Z. Bielecki, "Analysis of operation conditions of avalanche photodiodes on signal to noise ratio", *Opto-Electronics Review*, Vol. 5, pp. 249–256, 1997.
- [25] A. A. Mohamed, M. El-Halawany, Ahmed Nabih Zaki Rashed, and H. El-Hageen, "Harmful proton radiation damage and induced bit error effects on the performance of avalanche photodiode devices", *International Journal of Multidisciplinary Sciences and Engineering*, Vol. 2, pp. 27-36, 2011.
- [26] K. A. Murray, J. E. Kennedy, B. M. Evoy, O. Vrain, D. Ryan, D. Ryan, and C. L. Higginbotham, "Effects of gamma ray and electron beam irradiation on the mechanical, thermal, structural and physicochemical properties of poly (ether-block-amide) thermoplastic elastomers", *Journal of the Mechanical Behavior of Biomedical Materials*, Vol. 6, pp. 255-305, 2012.



**Author's Profile**

**Dr. Ahmed Nabih Zaki Rashed** was born in Menouf city, Menoufia State, Egypt country in 23 July, 1976. Received the B.Sc., M.Sc., and Ph.D. scientific degrees in the Electronics and Electrical Communications Engineering Department from Faculty of Electronic Engineering, Menoufia University in 1999, 2005, and 2010 respectively. Currently, his job carrier is a scientific lecturer in Electronics and Electrical Communications Engineering Department, Faculty of Electronic Engineering, Menoufia university, Menouf. Postal Menouf city code: 32951, EGYPT.

His scientific master science thesis has focused on polymer fibers in optical access communication systems. Moreover his scientific Ph. D. thesis has focused on recent applications in linear or nonlinear passive or active in optical networks. His interesting research mainly focuses on transmission capacity, a data rate product and long transmission distances of passive and active optical communication networks, wireless communication, radio over fiber communication systems, and optical network security and management. He has published many high scientific research papers in high quality and technical international journals in the field of advanced communication systems, optoelectronic devices, and passive optical access communication networks. His areas of interest and experience in optical communication systems, advanced optical communication networks, wireless optical access networks, analog communication systems, optical filters and Sensors, digital communication systems, optoelectronics devices, and advanced material science, network management systems, multimedia data base, network security, encryption and optical access computing systems. As well as he is editorial board member in high academic scientific International research Journals. Moreover he is a reviewer member and editorial board member in high impact scientific research international journals in the field of electronics, electrical communication systems, optoelectronics, information technology and advanced optical communication systems and networks. His personal electronic mail ID (E-mail:ahmed\_733@yahoo.com). His published paper under the title "**High reliability optical interconnections for short range applications in high speed optical communication systems**" has achieved most popular download articles in Optics and Laser Technology Journal, Elsevier Publisher in year 2013.